Atomic Force Microscopy - An advanced physics lab experiment

II. Institute of Physics

The Faculty of Mathematics, Computer Science and Natural Sciences
at RWTH Aachen University

April 2014

Contents

Chapter 1

Introduction

Since the first realization of a scanning tunneling microscope in 1981 by Binnig and Rohrer [1], a variety of scanning probe techniques has been developed in surface science. In all these techniques, the surface of a sample is scanned linewise by a very sharp tip and the tip-sample interaction is recorded with spatial resolution. By means of an electronic, a map of this interaction $W(x, y)$ is created. The first application of such an interaction in scanning probe microscopy was the tunneling current (see introduction to the scanning tunneling microscopy experiment). The development of the scanning tunneling microscope (STM) has been rewarded with the Nobel prize for Binnig and Rohrer in 1986. During that year, Binnig *et al.* realized the first atomic force microscope (AFM). [2] It uses a microscopic cantilever beam which has a tip integrated at its free end. During scanning the sample with this tip, the interaction forces bend the cantilever. This deflection can be measured by different techniques. In extension of the STM, AFM can also be used on insulating substrates. The interaction itself can take effect through very different mechanisms: van der Waals forces, chemical interaction, electrostatics, magnetostatics, capacitance, conductivity, friction, and many more. Depending on the design of the instrument, a spatial resolution down to the atomic scale and below can be achieved. A few of these interactions will be exploited during this experiment.

It is the goal to familiarize with the broad application range of this method and to study the imaging process as well as to identify different interactions giving rise to the contrast in a particular image. We will use topographic imaging in contact and tapping mode and magnetic and electrostatic force microscopy. The instrument is a commercial AFM with optical detection of the cantilever deflection.

This script shall only provide the most basic aspects concerning atomic force microscopy and how to conduct the experiment. For further informations about theory and applications of scanning probe microscopy the reader may refer to Ref. [3] and to [4] for a very specific theoretical description of tapping mode AFM.

Chapter 2

Forces

When two macroscopic objects are brought to close proximity, forces arise with different orders of magnitude and distance dependences. Under certain circumstances, these properties can be used to separate their respective contributions. Some of these forces, e.g., magnetic and electrostatic forces, can be manipulated by external fields or by voltage application. Thus, many physical properties of the sample can be measured with spatial resolution. Imaging the topography is only one possiblility. In this section, the forces relevant to atomic force microscopy will be discussed.

2.1 Van der Waals interaction

The van der Waals interaction describes atoms and molecules being attracted by respectively induced electric dipole moments. Even in a fully occupied electronic orbital, the dipole moment vanishes only when averaged over sufficiently long times. However, moments fluctuating on shorter time scales can polarize neighboring atoms. This mechanism leads to an attractive interaction potential $V_{\mathrm{vdW}} = -C/r^6$. When the distance is decreased further, repulsion of the atoms sets in due to the Pauli exclusion principle which can be tentatively described by a distance dependence $\propto r^{-12}$. The sum of these contributions is named Lennard-Jones potential and describes the interaction between two atoms separated by the distance r:

$$V_{\mathrm{LJ}} = -\frac{C}{r^6} + \frac{B}{r^{12}} \,. \tag{2.1}$$

A typical graph of V_{LJ} is depicted in Figure 2.1. In order to calculate the total force acting on a tip at distance x_0 above the sample, one has to sum up the contributions of all pairs of atoms. If we first neglect the atomic structure of the sample, we can replace the sum by an integral and the number of atoms per volume, ρ_s. An atom at distance r above the sample surface thus feels an attractive potential[1]:

$$V_{\mathrm{atom-sample}}(r) = -\frac{\pi C \rho_s}{r^3} \,. \tag{2.2}$$

[1] The repulsive part is only important in contact and is neglected here.

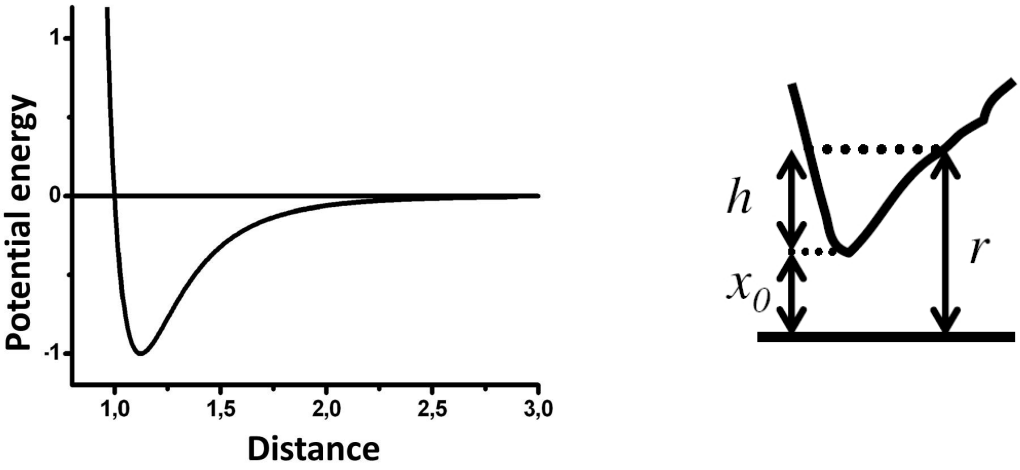

Figure 2.1: Van der Waals interaction. Left: schematic Lennard-Jones potential in arbitrary units. Right: variables used to describe the tip at a distance x_0 above the sample.

All atoms of the tip at the same distance contribute equally to the total potential. Thus, we can integrate over the cross section $A(h)$ of the tip [5], neglecting also the atomic structure of the tip:

$$V_{\mathrm{ts}} = -\frac{\pi C \rho_s \rho_t}{6} \int_0^H \frac{A(h)}{(x_0 + h)^3}\, dh\,, \tag{2.3}$$

where H denotes the total height of the tip. The expression in front of the integral is also called Hamaker constant. The function $A(h)$ is detemined by the tip geometry; e.g., $A \propto h$ for parabolic tips and $A \propto h^2$ for concial tips. This leads to a stronger dependence on the distance for parabolic (or blunt) tips ($\propto x_0^{-2}$) in comparison to conical or pyramidal (sharp) tips ($\propto x_0^{-1}$) implying that the distance dependence of the force is determined by the tip shape.[2] The repulsive part of the Lennard-Jones potential, in contrast, is responsible for the forces in the contact regime. Here, also elastic properties play a role.

2.2 Chemical bonding

If a tip comes very close to a surface, corresponding to interatomic distances, it may happen that chemical bonds are formed like in the interior of the sample, especially when ultraclean surfaces are involved. However, non-saturated bonds are necessary on both sides which is only the case when tip and sample are prepared in vacuum. Under ambient conditions, all surfaces are covered by thin films of adsorbates providing a passivation of

[2] The distance dependence can be calculated by evaluating Eq. 2.3 for a particular tip shape and differentiating with respect to x_0 (approximation: $x_0 \ll H$).

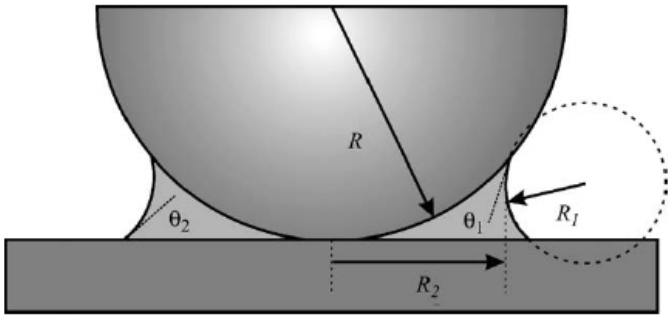

Figure 2.2: A water film on a sample under ambient conditions. A meniscus is formed between tip and sample. Taken from [6].

most of the surfaces. For our application, chemical forces can therefore be neglected. For investigations of ultraclean surfaces, they may be of great interest.

2.3 Water

A dominant contribution to the total forces in or shortly before contact is given by the presence of water. Every surface is covered by a film of water. The thickness depends on the humidity and can range from one up to several nanometers. In vicinity of a tip, a meniscus is formed (Fig. 2.2) which can totally dominate the forces between tip and sample in this regime. The deformation of the surface of the liquid causes a significant reduction of the local vapor pressure and leads to an enhanced condensation of water in the contact region, even at a humidity well below 100%. These pressure differences give rise to an energy gain when a meniscus is formed. There is also an influence of surface tension which is usually smaller [6]. Again, for the magnitude of capillary forces the tip shape is important. Blunt tips experience larger forces than sharp tips.

In nature, this effect is used by geckoes which can climb almost any wall, even on the bottom side of a glass plate. The reason are billions of spatulae, fine filaments which generate enough attractive force to the ground in order to hold the animal. A gecko can do it also in dry air but humidity helps [7] pointing towards contributions by van-der-Waals and capillary forces. This effect has been measured using an AFM cantilever with some spatulae glued to it (see Fig. 2.3).

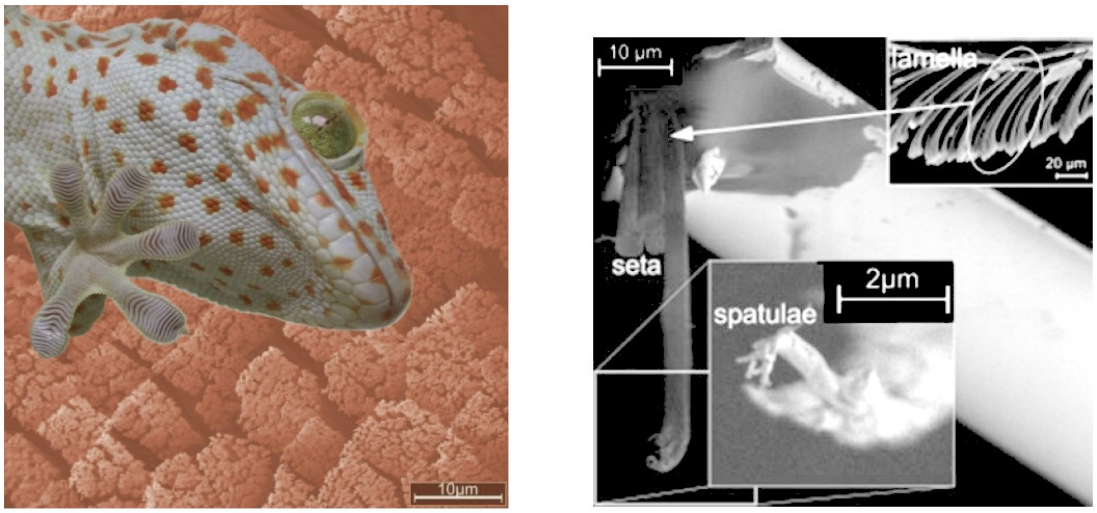

Figure 2.3: Links: Gecko holding on to a glass plate and microscopic image of the structure of the lamellae (background). Right: scanning electron microscopy image of a part of a lamella being glued to an AFM cantilever. Images taken from [7].

2.4 Contact

During AFM measurements under ambient conditions, contact between tip and sample is unavoidable in practically all types of measurement. Even when the cantilever is oscillating, the tip will hit the surface at the lower turning point. In this situation the tip is attracted towards the sample by the forces mentioned above. The tip end and the sample will locally be deformed until the attractive forces are compensated by elastic repulsive forces. The most basic assumption would be that, after contact, the tip feels a linear repulsive force according to Hooke's law: $F(z) = -k_{\mathrm{ts}} \cdot z$ for $z < 0$ and $F = 0$ otherwise; k_{ts} denotes a force constant representing the particular tip-sample interface. No adhesion and long range force are taken into acoount in this model. It turns out that this ansatz is by far not sufficient.

Next, we take into account the size of the contact area which increases with load force. A microscopic contact can be represented by a sphere of radius R pressed onto a plane with the presence of only elastic forces. [8] Lengthy calculations lead to a relation between normal load force F, the radius of the contact area a, and the tip movement δ normal to

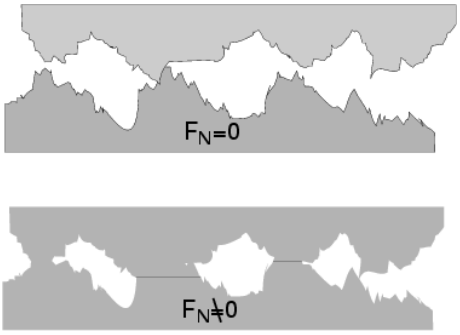

Figure 2.4: Microscopic model of two surfaces in contact. Taken from www.nano-world.org.

the surface:

$$a = \sqrt[3]{\frac{RF}{Y_{\text{total}}}} \tag{2.4}$$

$$\delta = \frac{a^2}{R} \tag{2.5}$$

$$\frac{1}{Y_{\text{total}}} = \frac{3}{4}\left(\frac{1-\nu_s^2}{Y_s} + \frac{1-\nu_t^2}{Y_t}\right). \tag{2.6}$$

The effective Young's modulus Y_{total} is combined from Young's moduli and Poisson's ratios of tip and sample. It is more complicated to take into account adhesion and distance dependent attractive forces. These contributions lead to a hysteresis of $F(z)$. The approaching tip snaps into contact below a certain distance and snaps off upon retraction only at a larger distance. Will will revisit this effect when force vs. distance curves are recorded.

2.5 Friction

If two macroscopic objects are moved with respect to each other under the influence of a normal load force, the friction force F_{R} is proportional to the load F_{N}, according to the well-known law of Amonton, $F_R = \mu F_N$. The frition force is in very good approximation independent on the macroscopic contact area. This law totally fails for microscopic contacts. Surprisingly, here the friction force does not depend on the load but is proportional to the area of contact. [9]

The exact mechanisms governing these empirical laws and especially the modelling of the transition from the microscopic to the macroscopic regime are still under investigation in a field called tribology. The most important aspect is that a real surface is never a perfect plane but consists of a large number of asperities (Fig. 2.4). Just a small fraction

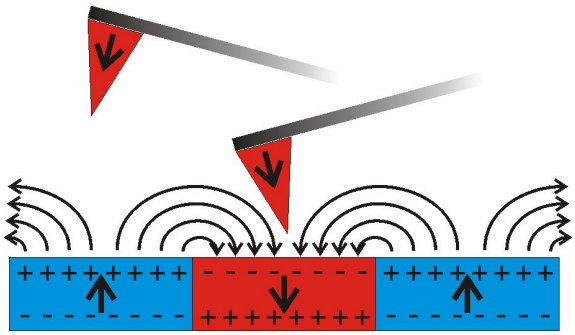

Figure 2.5: Magnetic tip above a ferromagentic sample with different domains. A stray field emanates from the sample surface which acts on the tip. Left: stray field and tip magnetization are antiparallel, resulting in a repulsive force. Right: parallel configuration of stray field and tip magnetization, attractive force.

of the surface really is in contact. Each microscopic contact contributes to the friction according to its area of contact and an increase of the load will mainly increase the number of microcontacts and thus the macroscopic friction force.

2.6 Magnetostatics

Magnetic structures can be imaged using magnetically coated tips. Figure 2.5 shows the basic principle. A magnetic tip is scanned above a sample which contains magnetic domains, i.e., regions in which the magnetization $\vec{M}$ is homogeneous. In our example, let the magnetization be perpendicular to the surface pointing upward or downward. From Mawell's equation $\vec{\nabla} \cdot \vec{B} = 0$, it follows that the normal component of $\vec{B}$ has to be continuous implying a non-zero field above the sample surface, called stray field. One can imagine this field caused by magnetic charges ρ_{mag} arising from a spatial variation of the magnetization: $\rho_{\mathrm{mag}} = -\vec{\nabla} \cdot \vec{M}$. However, one has to keep in mind that isolated magnetic charges do not exist and that the integral of ρ_{mag} over the sample volume has to vanish.

If the tip is positioned above a domain with the magnetization directed antiparallel to that of the tip (blue domain in Fig. 2.5) the stray field also is antiparallel to the tip magnetization. The tip feels a replusive force, and the cantilevers bends upwards. For parallel tip and sample magnetization, the tip is attracted.

A quantitative expression of the force can be obtained by regarding the tip as monopole. The tip dipole can be thought of being composed of two monopoles, one at the lower tip end and one at the upper one. Since the tip is normally much larger than typical domain sizes, only the lower monopole close to the surface sees the distribution of domains. The force acting on the upper monopole is an average over many micrometers and contains

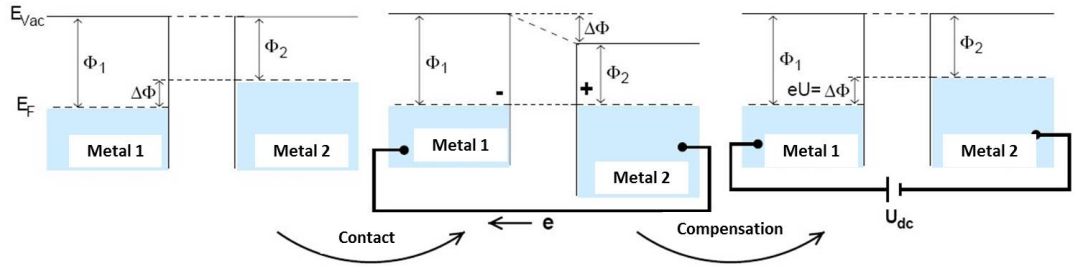

Figure 2.6: Contact potential difference. Left: Two uncharged, isolated metals share the vacuum level as commom energy level. Brought into contact, the Fermi energies equilibrate (mid), and a potential drop across the interface leads to an attractive force. A reverse bias applied between the two metals eliminates this force. Taken from [10].

nearly no spatial information parallel to the sample plane. The perpendicular force is then dominated by the monopole q at the lower tip end:

$$F_z = qH_z\,, \tag{2.7}$$

where H_z denotes the stray field in z direction. For the dynamic mode, the variation of the effective spring constant is important:

$$k' = \frac{\partial F_z}{\partial z} = q\frac{\partial H_z}{\partial z}\,. \tag{2.8}$$

Thus, in the dynamic mode of magnetic force microscopy predominantly the gradient of the sample stray field is imaged.

2.7 Electrostatics

The electrostatic attraction between tip and sample can be explained by a capacitor model. Let us consider a plate capacitor with capacitance C. The electrostatic energy of this capacitor charged with $Q = CU$ at a voltage U is $E = \frac{1}{2}CU^2$. Besides the geometry (area and shape of the plates), the capacitance depends on the distance z between the plates: $C = C(z)$. If we compute the derivative of E with respect to z, we obtain the force acting between the two plates:

$$F_{\mathrm{el}} = \frac{\partial E}{\partial z} = \frac{1}{2}\frac{\partial C}{\partial z}U^2\,. \tag{2.9}$$

A more complicated situation arises when material with different work functions are brought together. The work function Φ is the minimum energy needed for an electron to escape and thus is equal to the energy difference between Fermi energy and vacuum level (Fig. 2.6). Let us first consider two metals, electrically neutral and not connected (Fig.2.6(a)). In this case the common energy level is the vacuum level. Since the work

functions will be different in general, the Fermi energies are not identical. Only if these materials are brought into contact, electrons can move (in our case from metal 2 to metal 1) until the Fermi levels align (Fig.2.6(b)). Now, the vacuum levels above each material are shifted with respect to each other by the difference $\Delta\Phi$ of their work functions. $\Delta\Phi$ is called the contact potential difference. The gradient in the electrostatic potential of the vacuum level is nothing else than an electrical field $E \approx \Delta\Phi/d$ where d denotes the distance between the surfaces of the two materials. This field is caused by the transfer of electrons in order to achieve alignment of the Fermi energy and leads to an attractive electrostatic interaction between tip and sample. This interaction can be eliminated by applying a bias voltage of $U = \Delta\Phi/e$ (Fig.2.6(c)). Therefore, Eq. 2.9 has to be modified:

$$F_{\mathrm{el}} = \frac{\partial E}{\partial z} = \frac{1}{2}\frac{\partial C}{\partial z}(U - \Delta\Phi/e)^2 \,. \tag{2.10}$$

Electrostatic forces can significantly disturb images intended for magnetic imaging. Even in topography, this effect can lead to artifacts when materials with different work functions are scanned within the same image frame, e.g., thin film islands on a substrate.

The challenge of a quantitative evaluation of electrostatics in a scanning force microscope arises from the problem of finding the correct capacitance. For two metallic sides with high charge carrier density the charges are in very good approximation located directly at the surfaces. Here, the geometry detemines the capacitance. In semiconductors, however, not enough charge carriers are present to screen the electric field which then also penetrates into the bulk. Thus, depletion and accumulation zones arise associated with shifts of valence and conduction bands which are also known from *pn* junctions in diodes. The screening length is larger for smaller charge carrier density.[3] In semiconductors, the charge carrier density is in first approximation the number of dopants per volume. In general, a higher charge carrier density increases the capacitance due to the smaller depletion and accumulation zones which brings opposite charges closer together. Thus, scanning force microscopy offers the possibility of identifying areas of different doping levels. This may be of great interest in the semiconductor industry.

[3] Metals and insulators are two limiting cases of this picture. In metals, the screening length is of the order of atomic distances due to the high charge carrier density. In insulators, the screening length approaches infinity since there are no free charge carriers.

Chapter 3

Scanning force microscopy

The principle of scanning force microscopy is depicted in Figure 3.1. The sample s fixed on a holder which can be fine-positioned by a piezoelectric transducer *(scanner)* in lateral and vertical direction. Above the sample, a cantilever is mounted on another holder. Once the sample is scanned under the cantilever, the interaction between tip an sample causes the cantilever to bend. This deflection is a measure of the force acting on the tip and can be detected by deflection of a laser beam, by piezoelectric or piezoresistive sensors on the cantilever, or by interferometry.

This deflection signal - or interaction strength - can be used to control the tip-sample distance by moving the scanner *(feedback)*. Thus, a constant deflection can be set by the user and controlled automatically *(static mode)*. Another possibility is to oscillate the cantilever with its resonance frequency *(dynamic mode)*. In this mode, the change of oscillation properties is recorded as a measure of tip-sample interaction. Both of the modi will be used during the course of this experiment. In the following we will briefly review the most important components of a scanning force microscope.

3.1 Scanner

Most of the scanning probe microscopes use for the movement of the sample a piezoelectric element, often made of PZT (lead zirconium titanate). These are crystals which create an electric polarization when deformed mechanically due to their symmetry (polar axis). The reason is a movement of different atomic species in different directions within one unit cell. If the crystal shows a permanent electric polarization even without external pressure, it is called ferroelectric. The piezoelectric effect is reversible in the sence that an applied electric field will deform the crystal. In order to be useful as a scanner, the crystal has to be cut in a certain direction and coated with metallic electrodes. Then, a voltage applied to the electrodes will move the end of the scanner. Typical sensitivities are a few nm per volt, the right order of magnitude for a movement at the scale of atoms. Voltages up to a few 100 V are used during normal operation.

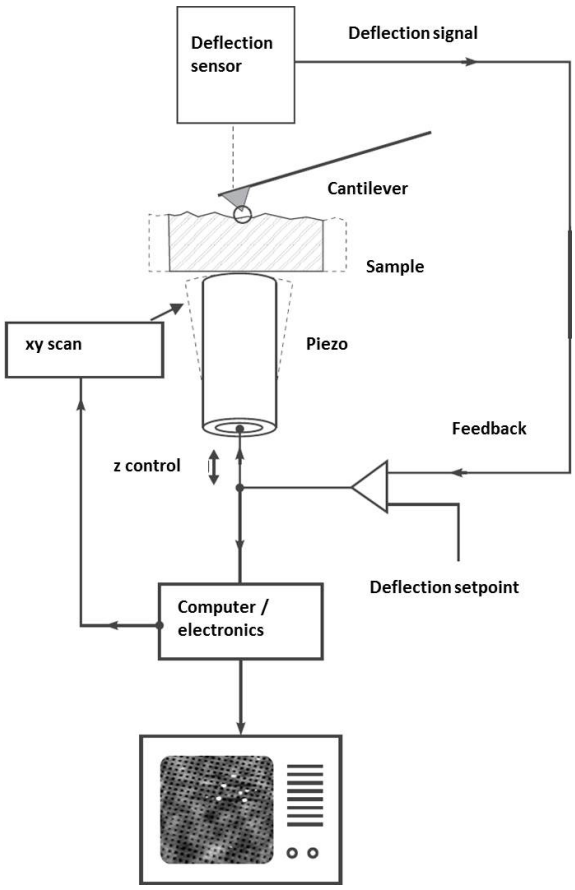

Figure 3.1: Principle of scanning force microscopy. During scanning, a feedback controls the deflection signal of a cantilever to be constant by changing the tip-sample distance accordingly. Deflection and feedback reaction are recorded electronically.

The simplest possibility of creating a threedimensional movement is the implementation of one piezo crystal per spatial direction. This is also the case in the AFM used in our experiment. Here, the lateral movement is increased to 30 μm by a lever arm construction.

Just like a ferromagnet, also ferroelectric materials exhibit a hysteresis. That means that the actual deflection of the scanner does not only depend on the voltage applied at the moment but also depends on the history of voltages applied before. Furthermore, the piezo reacts to a voltage step with a fast deflection followed by a slow relaxation, called *creep* which can last minutes, or even many hours at low temperatures. Additionally, there is thermal drift which is a slow irregular movement due to the movement of ferroelectric domain walls. These effects can substantially influence the image quality, especially after changes of the scan area.

In more recent alternative developments, instead of piezocrystals electromechanic devices are used similar to a hi-fi speaker. The position can be adjusted by passing a current

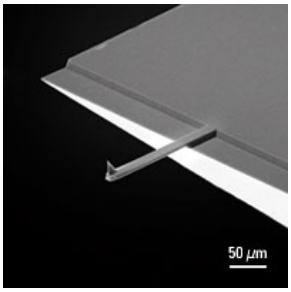

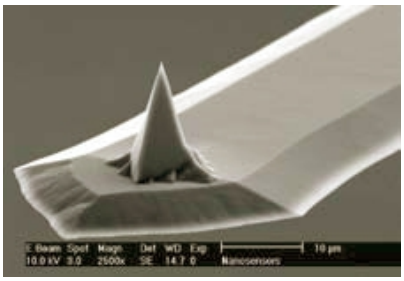

Figure 3.2: Scanning electron microscopy images of cantilevers. Left: Carrier chip with cantilever. Right: End of the cantilever with integrated tip. Taken from µmasch and Nanosensors company websites.

through a coil system with a magnetic element inside which is fixed to a membrane. Only small voltages are necessary. However, the heat generated by the current may reduce the stability of the system.

3.2 Cantilever

The tip, the cantilever and the carrier chip are fabricated from one piece of a wafer, typically silicon or silicon nitride, through various etching processes. Figure 3.2 shows two electron micrographs. The cantilever has a typical size of $200 \times 30 \times 5\,\mu\text{m}^3$ but can vary according to the desired properties such as spring constant or resonance frequency. At its end, an approximately $10\,\mu$m large tip is located. It can be modified further, i.e., by metal coating for electric or magnetic measurements, or by sharpening using ion bombardment or electron beam for better spatial resolution. The end of a typical untreated tip has a radius of several nm. A large variety of tips is commercially available.

The quantity most characteristic for a cantilever is the spring or force constant k. It can be detemined from the geometric dimensions (length L, width w, thickness t) and Young's modulus ($E = 110\,\text{GPa}$ for silicon) [11]:

$$k = \frac{Ewt^3}{4L^3} \tag{3.1}$$

Using the above mentioned dimensions, one calculates force constants in the order of several N/m. The resonance frequency f_0 is derived from the well-known expression for a harmonic oscillator, $(2\pi f_0)^2 = k/m^*$, modified by an effective mass $m^* = 0,2427\rho Lwt$:

$$f_0 = 0,1615 \cdot \frac{t}{L^2}\sqrt{\frac{E}{\rho}} \tag{3.2}$$

with $\rho = 2340\ \text{kg/m}^3$ being the density of silicon. In general, force constants are known

only approximately since a calibration of each cantilever would be very time-consuming. If one assumes that the greatest uncertainty arises from the thickness of the beam, one can try to estimate the force constant by eliminating the thickness and measuring the resonance frequency. Eliminating t from the above equations leads to:

$$k = 59,32 w L^3 f_0^3 \sqrt{\frac{\rho^3}{E}}\,. \tag{3.3}$$

By comparison between the nominal and measured resonance frequencies, one can estimate the actual force constant.

3.3 Detection of the cantilever deflection

In order to determine the force acting between cantilever and sample, one has to measure the deflection of the cantilever. In the first implementation of a scanning force microscope, a tunneling tip was placed on a second piezo above the cantilever. Following the principle of the scanning tunneling microscope invented a few years before, the tunneling current was kept constant by a feedback. From the necessary deflection of the second piezo, the cantilever deflection was determined. This setup needs basically two microscopes in one and is terribly complicated to operate. In addition to the tip adjustment, contaminations on the backside of the cantilever are critical as well as force interactions between tunneling tip and cantilever. This technique has not been successful, as one can imagine.

An attractive approach is to measure the deflection by the cantilever itself. There are basically two possibilities: piezoresistive and piezoelectric. The **piezoresistive** detection makes use of the resistance change of certain material (e.g., silicon) upon strain. This change can be measured using a resistance bridge. This setup is very compact. However, passing a permanent current through the cantilever produces heat in the device with resulting noise and thermal instabilities.

The **piezoelectric** detection is inverse to the creation of the scanning motion. The cantilever deflection causes an electrical polarization which can be measured by electrodes at both sides of the cantilever, either as current or voltage. Since the charges involved are very small and can be easily dimished by leak currents, this method is only suitable for oscillating cantilevers. An important example of this technique is the quartz tuning fork which is also used in quartz watches. At the end of such sensor, almost arbitrary tips can be mounted. Using this technique, a remarkable quality of atomic resolution imaging has been achieved in recent years.[1]

[1] www.physik.uni-regensburg.de/forschung/giessibl

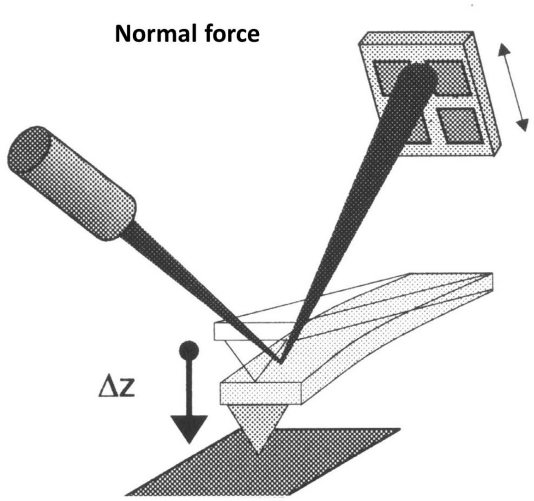

Figure 3.3: Optical beam deflection. A laser beam is deflected from the cantilever towards an array of photodiodes. The intensities are converted into vertical deflection and torsion of the cantilever. Image taken from Ulm University.

The most common detection scheme is the **optical beam deflection** (Fig. 3.3) which is also used in our setup. A laser beam emitted by a laser diode is directed onto the cantilever and reflected onto an array of four photodiodes. By subtracting opposite diode signals, the vertical deflection and also a torsion of the cantilever can be detected. This is especially interesting for friction forces. No other detection scheme can offer the simultaneous acquisition of two deflection channels. A disatvantage might be interference by laser light reflected from the sample surface.

Another common optical technique is the **interferometric detection**. Here, the end of a glass fiber which carries the laser light is approached towards the backside of the cantilever. The end of the fiber is cut with a special tool in order to produce a partially reflectign cleavage plane. This fiber end and the cantilever now form an interferometer: a part of the beam is reflected at the fiber end, another at the cantilever. The resulting interference signal depends on the cantilever-fiber distance and serves as a relative measure of deflection. This technique is used for microscopes operating in vacuum and at low temperatures where the signal has to be carried optically towards an electronic outside of the chamber. On the other hand, the fiber end has to be approached up to a few μm towards the cantilever which means additional effort in adjustment. Together with the quartz tuning fork, this detection scheme provides the best results in terms of stability and resolution.

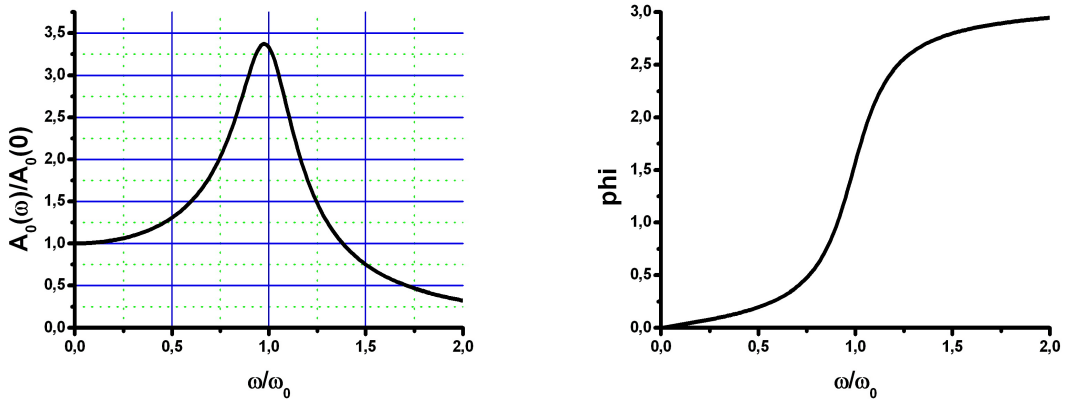

Figure 3.4: Amplitude and phase resonance curves of a damped, driven harmonic oscillator.

3.4 Harmonic oscillator

The motion of the cantilever and its reaction to an external force field can be described in a good approximation by a damped and driven harmonic oscillator. Therefore, the basic aspects shall be repeated here.

A harmonic oscillator is characterized by the parameters mass m, force constant k, and damping coefficient λ. In a static force, the oscillator is deflected by $\Delta x = F/k$. If the oscillator is driven by a periodic, sinusoidal external force, the equation of motion reads:

$$m\ddot{x} + \lambda\dot{x} + kx = C_0 \cos(\omega t)\,. \tag{3.4}$$

The Ansatz $x(t) = A_0 \cos(\omega t - \varphi)$ (or complex) yields the amplitude and phase resonance curves (3.4):

$$A_0(\omega) = \frac{C_0/m}{\sqrt{(\omega_0^2 - \omega^2)^2 + (2\gamma\omega)^2}} \tag{3.5}$$

$$\tan\varphi = \frac{2\gamma\omega}{\omega_0^2 - \omega^2} \tag{3.6}$$

with $\omega_0^2 = k/m$ and $\gamma = \lambda/2m$. For weak damping ($\gamma \ll \omega_0$), the resonance frequence resulting in the maximal amplitude is $\omega_{\text{res}}^2 = \omega_0^2 - 2\gamma^2 \approx k/m$. Often the mechanical quality factor $Q = \omega_0/2\gamma$ is used. After Q oscillations, the amplitude of the free oscillation is reduced be the factor $e^{-\pi} \approx 0,043$. The height of the resonance is $A_0(\omega_{\text{res}})/A_0(\omega = 0) = Q$ and the width $(A_0(\omega)/A_0(\omega_{\text{res}}))^2 = 1/2 \Leftrightarrow \Delta\omega/\omega = 1/Q$. A high Q means a sharp and high resonance. After starting the excitation, the system needs a time in the order of Q/f_0 until it reaches a steady state oscillation. Cantilevers in air exhibit a Q factor of several

100, in vacuum it can rise up to 10^5.

Now we want to extend the equation of motion to a distance dependent force $F(x)$:

$$m\ddot{x} + \lambda\dot{x} + kx = C_0 \cos(\omega t) + F(x)\,. \tag{3.7}$$

Additionally, we assume that the force is small compared to the restoring force of the cantilever and that the force varies only slightly at the scale of the oscillation amplitude, regarding the force as "long range". Under these assumptions, the oscillation will stay approximately harmonic and we can write down a Taylor expansion around the zero deflection point of the cantilever: $F(x) \approx F(x_0) + \frac{\partial F}{\partial x}\Big|_{x=x_0} \cdot x + \ldots$ um x_0. We now define

$$k' = \frac{\partial F}{\partial x}\Big|_{x=x_0} \tag{3.8}$$

and substitute this expression into the equation of motion:

$$\begin{aligned} m\ddot{x} + \lambda\dot{x} + kx &= C_0 \cos(\omega t) + F(x_0) + k'x \\ m\ddot{x} + \lambda\dot{x} + (k - k')x &= C_0 \cos(\omega t) + k \cdot \delta x \end{aligned} \tag{3.9}$$

With $k_{\text{eff}} = k - k'$ and $k \cdot \delta x = F(x_0)$ and a shift of the origin by δx corresponding to a static deflection of the cantilever we can again arrive at the original form of the equation of motion:

$$m\ddot{x} + \lambda\dot{x} + k_{\text{eff}}x = C_0 \cos(\omega t)\,, \tag{3.10}$$

only with the modification that the new force constant k_{eff} now contains the tip-sample interaction and thus depends on the tip position and on the distance.

The new effective force constant leads to a new resonance frequency f' of the cantilever:

$$\omega' = 2\pi f' = \sqrt{\frac{k_{\text{eff}}}{m}} = \sqrt{\frac{k - k'}{m}} \approx \sqrt{\frac{k}{m}}\left(1 - \frac{1}{2}\frac{k'}{k}\right) = \omega_0\left(1 - \frac{k'}{2k}\right)\,. \tag{3.11}$$

Thus, the resonance frequency has been shifted by the amount

$$\Delta f = f' - f_0 = -\frac{f_0}{2k}\,\frac{\partial F}{\partial x}\Big|_{x=x_0}\,. \tag{3.12}$$

For an attractive potential, $\partial F/\partial x > 0$ and $\Delta f < 0$, for a repulsive potential, $\Delta f > 0$. Therefore, a long-range force results in a frequency shift and a shift of the resonance curves, proportional to the force gradient between tip and sample. On the other hand, a constant force with respect to the distance does not produce a frequency shift but only a static deflection. Typical resonance curves for an attractive potential are shown in Fig. 3.5. An AFM measurement in the dynamic mode uses an amplitude which is held constant by a

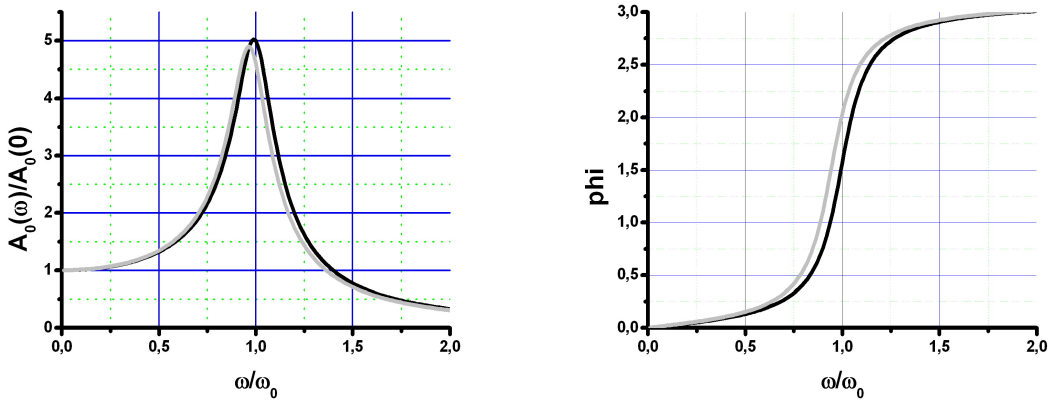

Figure 3.5: Amplitude and phase resonance curve of a damped, driven harmonic oscillator without (black) and with (grey) attractive force.

feedback which adjusts the distance. The phase is recorded independently by a Lock-in amplifier.

3.5 Feedback

The standard mode of AFM operation (in contact mode) is imaging with a constant deflection of the cantilever, or constant force. To this end, the sample has to be moved towards or away from the cantilever by means of the z piezo, according to the topography of the sample. This is done by a feedback which compares the actual deflection signal I with a setpoint S chosen by the user. From the deviation, or error signal $E = I - S$, the motion Δz of the piezo is calculated. Often, a PID (proportional, integral, differential) feedback controller is used. It can in general be described by

$$\Delta z(t) = g_p E(t) + g_i \frac{1}{T_I} \int_{t-T_I}^{t} E(\tau)\, d\tau + g_d T_D \frac{dE(t)}{dt}\,. \tag{3.13}$$

The first term is the proportional part which translates the error directly into a correction. For the integral part, the error is accumulated over a time T_I meaning that variations faster than T_I have a diminished effect on the corection. The third term, the differential part, reacts especially on fast changes of E, e.g., arising from step edges in the topography. In general, larger amplification factors g lead to a faster reaction of the feedback. Figure 3.6 shows the reaction of the feedback to an ideal step in the topography for different feedback sensitivities g. If these factors are too small the feedback does not follow the topography well. For larger sensitivities, there is danger of overshooting.[2]

[2] See also the manual for scanning tunneling microscopy.

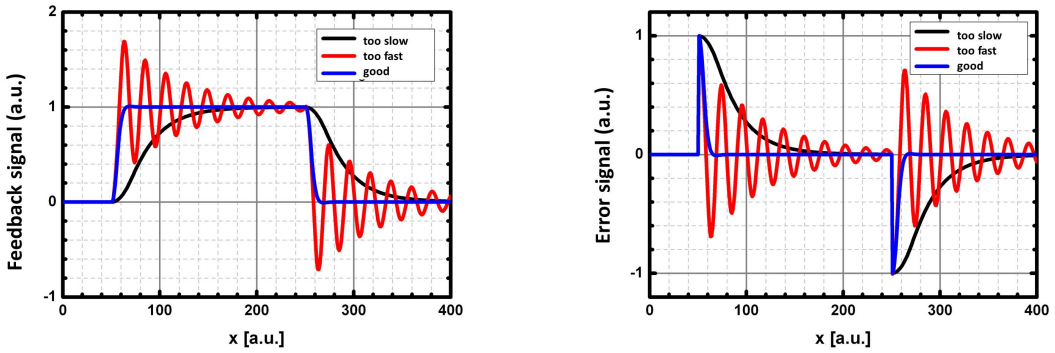

Figure 3.6: Examples of the feedback reaction to an ideal step in the topography. Left: feedback signal (e.g., the voltage applied to the z piezo). Right: error signal (e.g., the cantilever deflection or oscillation amplitude). If the amplification factors are too small (black), the feedback need too much time to accurately follow the step height. For a too high sensitivity (red), overshooting and oscillations occur.

In real feedbacks, things are more complicated due to additional time constants intrinsic to the electronics and the digitization procedure. In any case, looking at the error signal is a great help in judging if the feedback parameters are properly set. In our case, the error signal is the cantilever deflection in the static mode and the amplitude in the dynamic mode. Overshooting results for example in wave patterns and a slow feedback will translate image components of the topography into the error signal channel.

3.6 Lock-in amplifier

An AFM may be operated not only in the static but also in a dynamic mode. Here, the cantilever is driven by a sinusoidal signal and the amplitude and phase of the oscillation with respect to the driving signal is measured. This is done by using the lock-in technique which is frequently used in order to amplify weak signals. In a weak signal, noise of broad frequency range will contribute significantly, so the interesting signal has to be filtered from the noise. The trick is to modulate the signal with a known frequency, to measure the signal only at this frequency and to ignore other components in the frequency domain.

Take for example a signal of frequency f_0 which is superimposed by a noise signal of another frequency f_s:[3]

$$S(t) = A_0 \cos(2\pi f_0 t) + A_s \cos(2\pi f_s t)\,. \tag{3.14}$$

[3]The real noise can be decomposed into different frequencies. In this case you can take the amplitude at frequency f_s as Fourier component of the noise.

Let us now multiply this signal by a reference oscillation $R(t) = \cos(2\pi f_0 t)$ of the same frequency as the desired signal:

$$\begin{aligned} R(t) \cdot S(t) &= A_0 \cos^2(2\pi f_0 t) + A_s \cos(2\pi f_0 t) \cos(2\pi f_s t) \\ &= \frac{A_0}{2} + \frac{A_0}{2} \cos(4\pi f_0 t) \\ &+ \frac{A_s}{2} \cos(2\pi(f_0 + f_s)t) + \frac{A_s}{2} \cos(2\pi(f_0 - f_s)t)\,. \end{aligned} \tag{3.15}$$

Here, we used the identity $\cos^2 \alpha = \frac{1}{2} + \frac{1}{2} \cos 2\alpha$. Now we determine the time average by intergrating over a finite time T:

$$\begin{aligned} X_{\mathrm{LI}} = \frac{1}{T} \int_0^T R(t) \cdot S(t)\, dt &= \frac{A_0}{2} + \frac{A_0}{T \cdot 8\pi f_0} \sin(4\pi f_0 T) \\ &+ \frac{A_s}{T \cdot 4\pi(f_0 + f_s)} \sin(2\pi(f_0 + f_s)T) \\ &+ \frac{A_s}{T \cdot 4\pi(f_0 - f_s)} \sin(2\pi(f_0 - f_s)T)\,. \end{aligned} \tag{3.16}$$

The contribution of the desired signal, $A_0/2$, remains constant while the influence of the noise is proportional to $1/T$ and is suppressed with greater T. For $T \to \infty$, only the part of S remains which oscillated at the same frequency as R. By looking at the last term we find that frequencies close to the reference frequnecy are being damped less effective. Now, the real signal will be a mixture of different frequencies but that does not diminish the effectiveness of this technique.

In general, there will be also a phase shift ϕ between the desired signal and the reference signal which has to be determined by an independent procedure: If two reference signals are used which are phase-shifted by 90°, $R_1 = \cos(2\pi f_0 t)$ and $R_2 = \sin(2\pi f_0 t)$, one can obtain two integrals X_{LI} and Y_{LI}, in analogy to Equation 3.15. From these integrals, one can calculate the amplitude A as well as the phase ϕ of the desired signal with respect to the reference signal:

$$A = \sqrt{X_{\mathrm{LI}}^2 + Y_{\mathrm{LI}}^2} \tag{3.17}$$

$$\tan \varphi = \frac{Y_{\mathrm{LI}}}{X_{\mathrm{LI}}}\,. \tag{3.18}$$

In the dynamic mode, the cantilever is driven near its resonance frequency. This excitation signal plays the role of the reference R. The cantilever answers with an oscillation being measured by the photo diodes. This mesurements is prone to noise, e.g., noise in the photo diodes or thermal oscillation of the cantilever. By means of lock-in technique, these distortions can be suppressed and the amplitude and phase of the cantilever oscillation

with respect to the driving signal can be determined. How an interaction force affects these signals is explained in Sect. 3.4.

Chapter 4

Methods

A scanning force microscope can be operated in different modi. Which method offers the best sensitivity depends on the nature of the interaction which is to be imaged. In this chapter, three methods shall be reviewed: measuring in contact with static cantilever deflection, the dynamic mode, and the fly mode which measures oscillation properties in a distance from the sample surface.[1]

4.1 Contact mode

The contact mode is the simplest operation mode of an AFM. The sample is approached towards the tip until the tip hits the surface and the cantilever is deflected. Larger deflection Δz means larger load force: $F_c = k \cdot \Delta z$. In setting the deflection of the cantilever for a measurement, one can select a particular load force, provided the force constant k is known. To the total force, also the adhesion force F_{adh} contributes which arises, e.g., from a water film or the attractive part of the van der Waals interaction: $F_{\mathrm{total}} = F_{\mathrm{adh}} + F_c$. Thus, the cantilever deflection gives only a lower boundary of the actual force acting on the tip-sample contact.

[1] For an overview of different other scanning probe techniques, see also http://www.ntmdt.com/spm-principles.

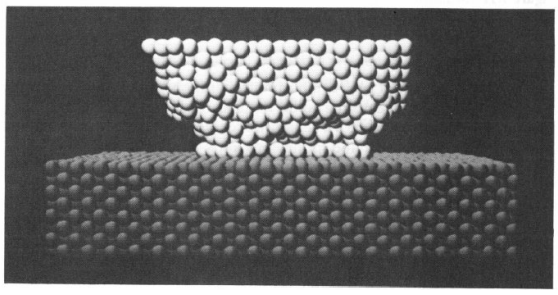

Figure 4.1: Simulation of a tip being in contact with the sample. The interface consists of up to several 100 atoms.

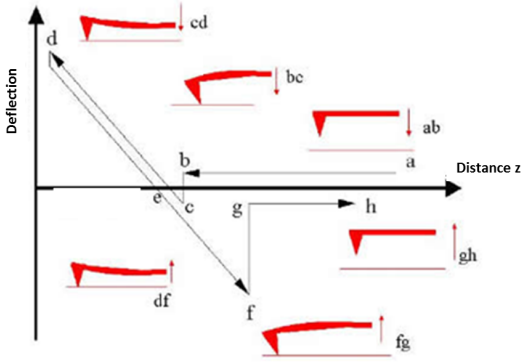

Figure 4.2: Schematics of a force vs. distance curve. At $b - c$ the tip snaps into contact due to the increasingly atrractive forces. Beginning in c up to position f the tip is in contact with the sanple and the deflection of the cantilever follows directly the cange of the piezo position z. At f, the restoring forces of the cantilever are equal to the adhesion forces. At $f - g$, the tip snaps back from the surface into its free position which is between $g - h$ and $a - b$ only influence by long-range van der Waals forces, with minimal bending of the cantilever.

In the contact mode, the contact area consists of a few 100 atoms (Fig. 4.1) which makes a true atomic resolution impossible. Due to the persistent contact and the tip moving sideways, the interface will be subject to wear and the tip will become blunt after some time. This effect can also be useful for measuring the friction force by evaluating the torsion of the cantilever. Another disadvantage is that the tip has the tendency to simply push away small object which may cover the surface. The contact mode is therefore not useful to judge the cleanliness of a sample. Due to the direct relationship between deflection and topgraphy, this method is suited for camparatively fast scanning.

4.2 Force-distance measurements

An important method for measuring the forces occuring in the contace mode are force-distance curves. This can be done by evaluating the cantilever deflection Δz and its force constant k by using $F = k \cdot \Delta z$. A typical sequence is shown in Fig. 4.2. When the sample approaches the tip, the attractive forces increase and the cantilever is slightly deflected. At smaller distances, the attractive forces increase faster than the restoring force of the cantilever ($dF/dz > k$) which makes it impossible to stabilize the tip in that regime. Instead, the tip snaps into the surface until full contact is established. After the snap-in, the tip moves in the same way as the sample and the cantilever is deflected linearly with the sample motion. Upon retracting the sample, the tip again follows the sample motion until zero deflection is reached. Here, the load force is zero but the adhesion forces are still present and hold the tip on the sample. Only when the cantilever is further retracted such that the restoring force is greater than the adhesion forces ($k \cdot \Delta z > F_{\mathrm{adh}}$), the tip

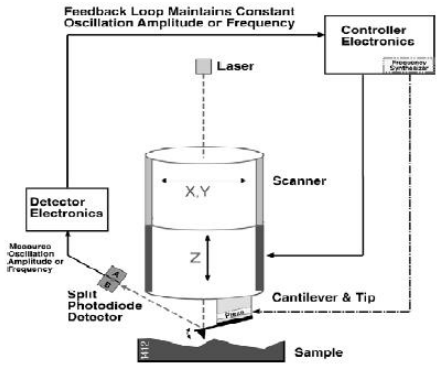

Figure 4.3: Dynamic mode: the cantilever is excited to a driven oscillation. The amplitude is taken as error signal and is held constant by changing the piezo's z position.

snaps back from the sample, and the cantilever is nearly in its zero position.

4.3 Dynamic mode

In the dynamic mode (other names: intermittent contact or tapping mode), the cantilever is excited to an oscillation at or near its resonance frequency. This is usually done by a small piezo element mounted below or directly on the cantilever holder. Typical amplitudes of a few tens of nm are achieved. The excitation (frequency and amplitude) is kept constant during the whole image. The observed quantities are the oscillation amplitude and phase of the cantilever with respect to the excitation. Both of them are determined from the deflection sensors with the help of an integrated lock-in amplifier (see Sect. 3.6). Figure 4.3 shows the signal diagram.

During approach of tip and sample, the amplitude slowly decreases over a distance of a few μm due to air damping and a slight frequency shift caused by long-range interactions. Once the tip hits the sample at the lower turning point, the amplitude suddenly decreases considerably. This drop can be used as a feedback signal for the distance by selecting an amplitude setpoint, e.g., 85% of the amplitude of the freee oscillation. At a distance which is too small, the amplitude is further reduced, and the feedback has to increase the distance by moving the z piezo while at too large amplitude, the distance has to be decreased.

In this mode, the tip hits the sample at every oscillation cycle. One can imagine that also the elastic properties influence the imaging process. Especially the phase (since the amplitude is kept constant by the feedback) shows often additional contrast which can be used to identify different materials such as a graphene sheet lying on a substrate. This effect can also cause the apparent height to be different from the physical height. The

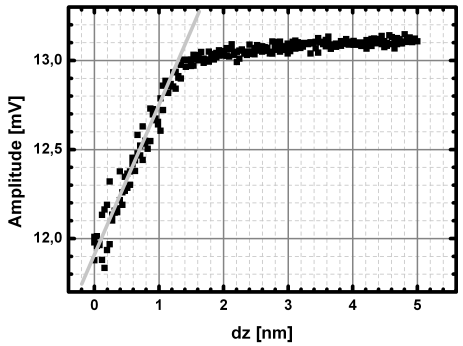

Figure 4.4: Distance-dependent amplitude. In the left part ($z < 1,4\,\text{nm}$), the tip hits the sample and the amplitude decreases linearly with the z movement of th sample. For greater distances, the combination of air damping and frequency shift (attractive interactions) leads to a slow change of the amplitude.

uncertainty when scanning different materials in one image can easily be of the order of an atomic layer.

In order to achieve an accurate height measurement, the oscillation has to be stabilized at every pixel. This needs a time constant Q/f_0 (s. Sect. 3.4) for the harmonic oscillator and another time constant which is the integration time of the lock-in. Therefore, the dynamic mode is slower than the contact mode.[2] However, the images normally show more details due to the smaller contact area and the effects of pushing away adsobates is greatly reduced.

4.4 Amplitude-distance curves

The direct proof that the tip hits the sample in the tapping mode is visible in a measurement of the amplitude with respect to the z position of the sample (Fig. 4.4). With decreasing distance, the amplitude changes slowly due to air damping close to the sample and due to a shift of the resonance frequency to lower values because of long-range van der Waals interactions. Once the tip hits the sample, the amplitude reduces approximately by the same value as the distance. If one assumes this linear relationship, one can approximately determine the absolute amplitude, even if the deflection signal itself (mV scale at the lock-in output) is not calibrated, provided the calibration of the z piezo is known.

[2] Using a mechanical $Q = 250$ and a frequency of 70 kHz, an image with 512×512 pixels needs at least 15 min.

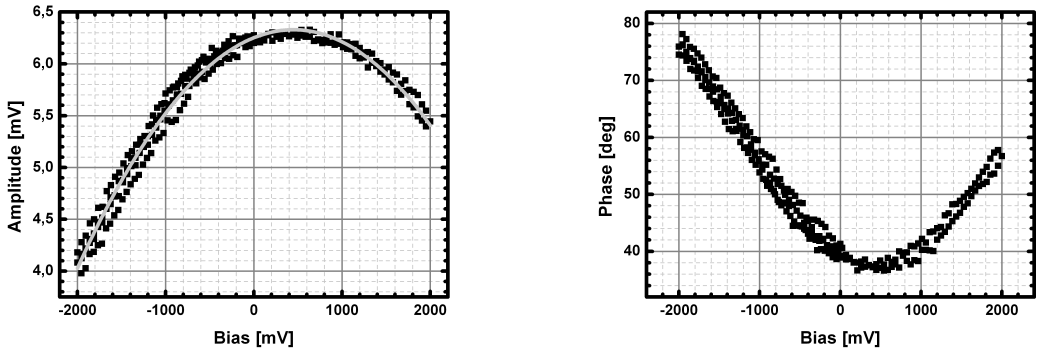

Figure 4.5: Amplitude (left) and phase (right) of a Cr-coated tip, dependent on the applied bias voltage. The parabolic fit (straight line) yields a contact potential difference of 450 mV.

4.5 Amplitude-voltage curves

The effect of electrostatics can be demonstrated by varying the tip-sample or bias voltage U. Hereby, the amplitude and phase are recorded. An attractive force due to the voltage will pull the tip towards the surface and thereby further reduce the amplitude. At the same time, the phase will change due to the changed attractive interaction. A typical curve is shown in Figure 4.5. According to Eq. 2.10 this additional force is proportional to $(U - \Delta\Phi/e)^2$. This contribution vanishes when $U = \Delta\Phi/e$. This voltage should be applied when it is advisable to eliminate electrostatic interaction, e.g., in magnetic force microscopy.

4.6 Fly mode

The fly mode (or lift mode) serves as a possibility to measure long-range forces. In the methods explained so far, short-range foreces are dominating. These are obviously strongly connected with the topography of the sample. In order to measure electrostatic or magnetostatic interactions, this influence has to be minimized. This is possible by retracting the tip a few tens of nm from the surface and recording the oscillation in the field of the long-range forces. In this case, the amplitude will not change significantly since the oscillation still take place close to the resonance frequency. But the change of the phase is proportional to the force gradient (see Sect. 3.4). Since also the van der Waals force contains long-range components but is correlated with the topography, it is important to perform the measurement at a constant height above the surface. The trick goes as follows: The sample is imaged in the dynamic mode and the topography recorded. Afterwards, the tip is retracted to a greater height and the same height profile is scanned

again, measuring only the long-range part of the force. In order to reduce distance errors this procedure is applied line-wise and not for the complete image. The most important application of this method is the magnetic force microscopy.

Chapter 5

The Anfatec Level AFM

In this experiment, a scanning force microscope produced by the company Anfatec is used. The details of the setup and handling will be layed out at the day of the experiment. Here, only a quick overview shall be given.

5.1 Setup

Figure 5.1 shows a photograph of the AFM. The massive ground plate rests on a rubber mat. On the ground plate, the microscope is suspended from three rods by viton belts. This setup helps isolating the microscope from oscillations of the floor.

In the microscope body, the stepper motors for the coarse approach are located. They drive three threaded rods ("fine screws") on which the scan head is placed. The stepper motors can move the scan head including the cantilever in steps of roughly 1 μm towards the sample. The sample is placed on a magnetic holder on top of the scan piezos and is scanned under the cantilever during imaging. Additionally, there are screws on two sides for a rough lateral adjustment.

The scan head contains the cantilever with the deflection detection mechanism. Figure 5.2 shows the optical path. The laser beam leaves the laser diode and is directed through a lens to a mirror and onto the cantilever. The reflected beam hits a second mirror and is directed towards am array of four photo diodes. The intensity on the four quadrants is a measure of deflection ($I_{\text{top}} - I_{\text{bottom}}$) and torsion ($I_{\text{left}} - I_{\text{right}}$) of the cantilever. The optical path has to be readjusted for every new cantilever in order for the laser beam to hit the center of the diode array. This is done by four adjustment screws for moving the lens, the two mirrors and the diode array. The cantilever is clamped by a spring. Its position can be checked by a camera from the top. In this holder, the piezo actuator for the dynamic mode is integrated. The scan head is placed on the three threaded rods of the course approach.

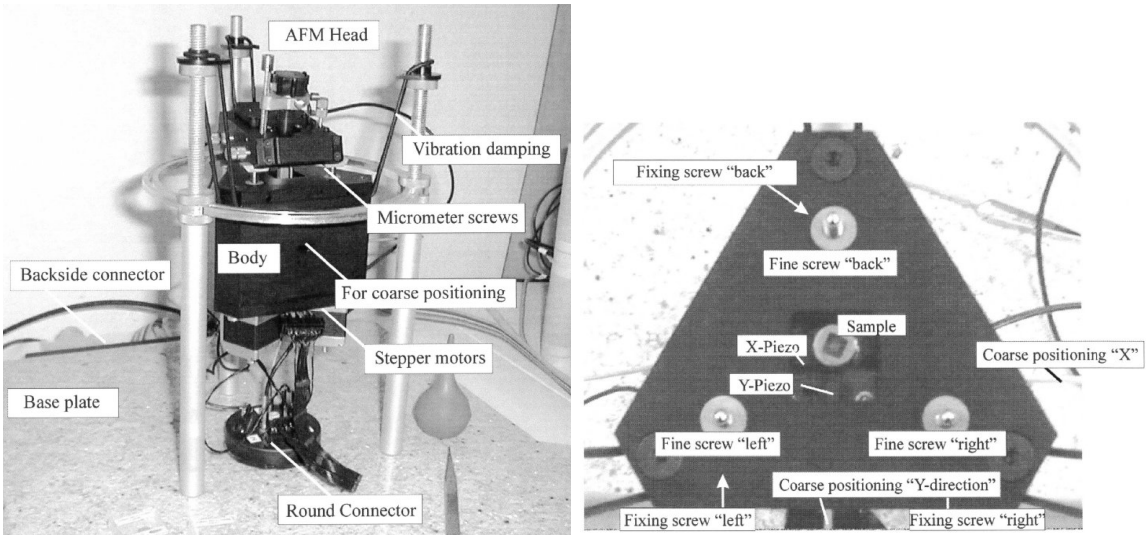

Figure 5.1: Left: Photograph of the Anfatec Level AFM. The microscope boy is suspended from viton belts for vibration isolation. The cantilever and the deflection detection (laser, photo diodes) are located in the the AFM head which is placed on the stepper motor screws for measurements. Right: The microscopy body (from above) containing the stepper motors for coarse approach and the sample holder with the scanning piezos.

The signals for scanning, deflection detection and oscilation are processed by a control electronics and directed to the PC and the scanning sofware. With this software, all data are acquired and the microscope is operated, except for the lateral coarse positioning.

5.2 Software

How to conduct the several parts of the experiment and the operation of the software will be explained by the tutor. Additionally there will be a comprehensive documentation available regarding the AFM. For a general overview, a few important features of the software shall be described here. Upon starting the software, the electronic should be already switched on. After inserting the cantilever and adjusting the laser beam, the control and fine adjustment is done via software.

5.2.1 Crosshairs

This window shows crosshairs which display the position of the laser beam on the photo diode array. By carefully turning the adjustment screws on the scan head, the laser should be centered to the crosshairs at highest amplification (gain 100). Also the intensity of the reflected beam can be read out as well as the deflection in x and y direction. These values

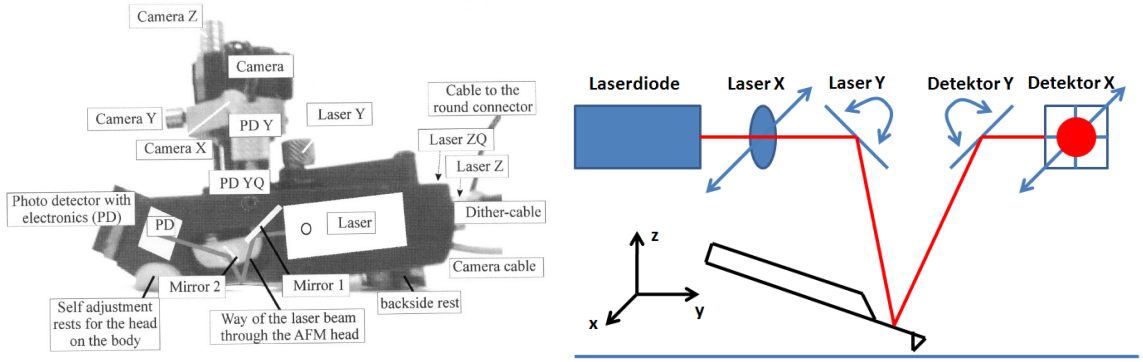

Figure 5.2: Left: Microscopy body. The laser beam is emitted by a laser diode and, after passing a lens, deflected towards the cantilever by a mirror. Passing a second mirror, the light hits the photo diode array. From above, the cantilever can be looked at using a CCD camera. The beam adjustment is done by turning screws for laser x,y and detector x,y.

are used in the software under the name T-B (top minus bottom) and L-R (left minus right).

5.2.2 Scan parameters

Here, the settings of the scan area (size, position, speed, number of pixels) and of the feedback are made.

- Ref.: denotes the setpoint S for the feedback. According to the respective mode of operation, it is the deflection (T-B) in contact mode or the amplitude (as percentage of the free oscillation, s. DNC window).

- K_i and K_p: feedback parameters. Using the deflection signal I and the setpoint S, the new position of the z piezo is calculated:

$$\Delta_{\text{neu}} = I - S \tag{5.1}$$

$$z_{\text{neu}} = z_{\text{alt}} + K_i \cdot \Delta_{\text{neu}} + K_p \cdot (\Delta_{\text{neu}} - \Delta_{\text{alt}}) \tag{5.2}$$

$$\Delta_{\text{alt}} = \Delta_{\text{neu}} \tag{5.3}$$

  In contrast to the naming, K_i resembles more the proportional gain and K_p the differential gain of the PID controller. An implicit integral part is given by the discrete time steps of the digital feedback. The manufacturer suggests to set $K_p = 3 \cdot K_i$ as a first guess.

- Bias: voltage applied to the sample with respect to the grounded tip.

- ◇ Alternative settings for the automatic approach: By right-click on K_i, K_p and bias, secondary values can be set which are only used during approach. While scanning the original settings are active again.
- ◇ Approach, retract: in the lower part of the menu the tip control is located. Right-clickling on the arrows opens a menu for different travel distances. The automatic approach can be started here as well.

5.2.3 Automatic approach

After the coarse approach of the tip towards the sample which is checked by eye, the final approach has to be done in an automated way. To this end, one activates the arrow pointing towards the sample in the menu "Scan Parameter". If the setpoint is not reached, the z piezo with the sample on top is elongated towards the tip. If no contact is estabiliched, the piezo is retracted again and the stepper motor moves a few μm forwards the tip (this distance has to be less than the z range of the piezo). Then the feedback is activated again and the piezo starts extending towards the tip again. The sequence is stopped automatically when the setpoint is reached.

5.2.4 Spectroscopy

In this window, different measurements performed at one position on the sample can be recorded, such as deflection, amplitude, phase, or lock-in signal dependent on distance or bias voltage. Start, end and speed of the ramps can be set.

5.2.5 DNC

The DNC (dynamic non-contact) window allows setting the cantilever excitation and measuring resonance curves. Values between 0.1 V and 1 V are recommended. Choosing the frequency and the amplitude setpoint is done by clicking into the graphical display of the resonance curve.

5.2.6 Other options

Furthermore, there are some more festures:

- ◇ Coarse move: for controlling the stepper motors.
- ◇ Oscilloscope: display of all signals in time or frequency domain.

- ◇ Feedback: here the signal used for the feedback can be selected; in static mode: deflection (T-B), in dynamic mode: amplitude (R).
- ◇ Acquire: selection of data channels to be recorded during the scan, such as deflection, topography, amplitude, phase, lock-in signal...

Chapter 6

Experiments and evaluation

6.1 Contact mode

The goal of this part is to get to know the microscope and the software. To this end, a sample with known properties is investigated: a test grid made out of silicon which is etched to form a stripe-like pattern with given period and step heights. This sample can be used for calibrating the piezo constants and for the investigation of image artifacts like piezo hysteresis and creep.

- ◇ mounting a contact mode cantilever (CSC17)
- ◇ adjusting the laser beam
- ◇ scanning of the test grid (topography, T-B, L-R) using different feedback parameters
- ◇ checking the piezo calibration

6.2 Force vs. distance curves

The force shall be estimated which attracts the tip towards the sample. The difference of snap-in and snap-off positions can be converted into forces by using the force constant of the cantilever.

- ◇ acquisition of force-distance curves
- ◇ determination of the resonance frequency and estimation of the force constant
- ◇ determination of adhesion force and load force from the curves and the force constant

6.3 Dynamic mode

In the dynamic mode, the roughness and potential contaminations can be evaluated. Due to the oscillation of the tip, it is much less likely to move away adsorbates. Before scanning, the appropriate excitation frequence has to be determined. A sample provided on the day of the experiment shall be examined with respect to the roughness and structure of the surface.

- ◇ mounting a dynamic mode cantilever (NSC15), adjustment
- ◇ determination of the resonance frequency
- ◇ imaging of a sample in the dynamic mode (topography, amplitude, phase)
- ◇ characterization of the surface (roughness, typical length scales, periodicities, preferred directions, contaminations)
- ◇ amplitude vs. distance curves
- ◇ estimation of the tip oscillation amplitude

6.4 Magnetic force microscopy

The magnetic domains of a hard disk shall be imaged.

- ◇ mounting of a magnetically coated cantilever (NSC18, CoCr)
- ◇ determination of the contact potential difference
- ◇ imaging the domain structure using the fly mode
- ◇ determination of the average domain size and the storage density in GBit/in^2

6.5 Evaluation and report

A suggested outline:

- ◇ goal of the experiment (max. 1 page)
- ◇ setup and principle of operation (short)
- ◇ description of required measurements and how they were conducted
- ◇ data evaluation and quantitative analysis

- ◇ discussion of results
- ◇ summary

The report shall not include:

- ◇ repetitive explanations taken from the manual
- ◇ superfluous descriptions of the course of the experiment or circumstances that have nothing to do with the results

For every required measurement and evaluation, appropriate images and data have to be presented und the steps of the evaluation and interpretation have to be clearly described. Every presented image has to be accompanied by the relevant parameters (area, modus, data channel, feedback settings) and other relevant information, dependent on the imaging method. An error has to be given for every quantitative result.

Chapter 7

Questions

After reading this manual, you should be able to answer the following questions:

- ◇ Which forces exist between two solid bodies of matter?
- ◇ How does an atomic force microscope work?
- ◇ Which modi of measurements exist?
- ◇ Which forces are dominant for the different modi?
- ◇ How does a distance dependent force change the model of a harmonic oscillator?
- ◇ How does a lock-in amplifier work?
- ◇ How does the distance-dependent deflection of the cantilever looks like in the static mode (approach and retract)?
- ◇ How can the oscillation amplitude of the tip be determined from amplitude vs. distance curves?
- ◇ Why is it in magnetic force microscopy more difficult to image domains with in-plane magnetization compared to out-of-plane?

Bibliography

[1] G. Binnig and H. Rohrer, Helv. Phys. Acta **55**, 726 (1982).

[2] G. Binnig, C. F. Quate, and C. Gerber, Phys. Rev. Lett. **56**, 930 (1986).

[3] R. Wiesendanger, *Scanning probe microscopy and spectroscopy* (Cambridge University Press, Cambridge, 1994).

[4] H. Hölscher and U. D. Schwarz, Int. J. Nonlin. Mech. **42**, 608 (2007).

[5] F. J. Giessibl, Phys. Rev. B **56**, 16010 (1997).

[6] H.-J. Butt, B. Cappella, and M. Kappl, Surf. Sci. Rep. **59**, 1 (2005).

[7] G. Huber, H. Mantz, R. Spolenak, K. Mecke, K. Jacobs, S. N. Gorb, and E. Arzt, P. Natl. Acad. Sci. USA **102**, 16293 (2005).

[8] H. Hertz, J. Reine Angew. Math. **92**, 156 (1881).

[9] R. W. Carpick, N. Agraït, D. F. Ogletree, and M. Salmeron, J. Vac. Sci. Technol. B **14**, 1289 (1996).

[10] C. Sommerhalter, *Kelvinsondenkraftmikroskopie im Ultrahochvakuum zur Charakterisierung von Halbleiter-Heterodioden auf der Basis von Chalkopyriten*, PhD thesis, Freie Universität Berlin, 1999.

[11] C. J. Chen, *Introduction to scanning tunnelling microscopy* (Oxford University Press, New York, 1993).